MULTIPHASE FLOW SIMULATION OF WAVE RUN-UP ON VERTICAL COLUMN UNDER WAVE ACTION

Koji KAWASAKI[1], Ut HAN DINH[2], Yoshitaka TAKASU[3]

[1]Member of JSCE, D. Eng., Associate Professor, Department of Civil Engineering, Nagoya University (Furo-cho, Chikusa-ku, Nagoya 464-8603, Japan)
[2] Nonmember of JSCE, M. Eng., Doctoral Student, Department of Civil Engineering, Nagoya University (Furo-cho, Chikusa-ku, Nagoya 464-8603, Japan)
[3] Student Member of JSCE, B. Eng., Master Student, Department of Civil Engineering, Nagoya University (Furo-cho, Chikusa-ku, Nagoya 464-8603, Japan)

海洋構造物を設計する際には，その周辺の波浪変形のみならず，構造物を遡上する波の特性も把握することが重要である．そこで，本研究では，規則波動場に設置された単一円柱構造物を対象に，固相－気相－液相の相互干渉が計算可能な3次元多相乱流数値モデルDOLPHIN-3Dを用いて3次元波浪計算を行った．計算結果と既往の水理実験結果の比較から本モデルの妥当性を検証し，本モデルが波と円柱構造物の相互干渉を良好に計算できることを明示した．また，規則波作用下における固定円柱構造物による波変形，円柱を遡上する波の特性を検討した．さらに，非固定円柱浮体構造物と波の相互干渉に関する計算を行うことにより，本数値モデルの固定構造物・非固定構造物への適用性を示した．

Key Words : *Wave run-up, multiphase flow, solid-gas-liquid interaction, extreme waves, numerical model*

1. INTRODUCTION

It is well known that the interaction between waves and columns of offshore structures causes rise of water surface above the level of the incident wave crests. When this occurs around the face of a column, it is defined as "run-up". In extreme waves, the amplification of the incident wave may give rise to impulse loads on the underside of the platform deck (referred to as "slamming") or may result in wave-in-deck, which damages the safety of equipment on the deck. This phenomenon therefore has serious consequences for platforms if it is not sufficiently understood and predicted. When wave run-up is overestimated, air gap can increase the fabrication cost and the overall weight of a platform, which affects the stability of platform structure. Conversely, an underestimation of the air gap can lead to slamming or wave-in-deck, which damages to platform.

Various studies have ever been conducted in order to estimate the extent of wave run-up for over the past six decades. MacCamy and Fuchs[1] solved this problem analytically by extending Havelock's linear potential theory. Extension of diffraction theory to the second order has been carried out by Kim and Yue[2], and Kriebel[3], [4]. Niedzecki and Duggal[5] employed a semi-empirical variation to determine wave run-up. Isaacson and Cheung[6] developed an integral equation method based on the Green's theorem to study a second order wave diffraction around two-dimensional bodies, nonlinear wave forces, and run-up on a surface piercing body of arbitrary shapes. The above-mentioned studies were found to be inadequate to analyze wave run-up in extreme waves because their assumption is that the motion of waves is moderate. Therefore, it is of extremely importance to discuss wave run-up on offshore structures in extreme waves as well as moderate waves from the perspective of structure design.

In the present study, wave run-up on vertical column is examined by using a three-dimensional (3-D) numerical model of multiphase flow with solid-gas-liquid phase interaction, which has no assumption used in the small amplitude theory. The model is verified by comparisons of numerical simulation results with the previous experimental ones. Additional examination reveals the capacity of the model for investigating interaction of wave and an unfixed body.

2. 3-D MULTIPHASE FLOW MODEL

(1) Governing equations

The governing equations consist of the conservation of mass (Eq.(1)), the Navier-Stokes equations (Eq.(2)), the pressure equation for compressible fluid (Eq.(3)), the advection equation of density functions (Eq.(4)) and the equation of state for barotropic fluid (Eq.(5)). The equations allow us to precisely compute not only incompressible but also compressible multiphase flows.

$$\frac{\partial \rho}{\partial t}+\frac{\partial (u_j \rho)}{\partial x_j}=\rho q \tag{1}$$

$$\frac{\partial u_i}{\partial t}+u_j\frac{\partial u_i}{\partial x_j}=-\frac{1}{\rho}\frac{\partial p}{\partial x_i}-g_i+\frac{f_{si}}{\rho} +\frac{\partial}{\partial x_j}\left(-\tau_{ij}+2\frac{\mu}{\rho}S_{ij}\right)-D_i u_i \tag{2}$$

$$\frac{\partial p}{\partial t}+u_j\frac{\partial p}{\partial x_j}=-\rho C_{ls}{}^2\left(\frac{\partial u_j}{\partial x_j}-q\right) \tag{3}$$

$$\frac{\partial \phi_I}{\partial t}+u_j\frac{\partial \phi_I}{\partial x_j}=0 \tag{4}$$

$$\rho=f(p) \tag{5}$$

$$q=\begin{cases}0 & (x\neq x_s)\\ q^* & (x=x_s)\end{cases} \tag{6}$$

where, x_i is position vector (x, y, z), u_i is velocity component in the direction of i, ρ is fluid density, p is pressure, g_i is gravitational acceleration vector (0, 0, -g), f_{si} is surface tension term, τ_{ij} is turbulence term, μ is the coefficient of viscosity, S_{ij} is strain rate tensor ($\partial u_i/\partial x_j+\partial u_j/\partial x_i$), D_i is dissipation coefficient used in added dissipation zone, C_{ls} is local sound speed, t is time and ϕ_I (I =1 ~ 3) are density functions for respective phases (ϕ_1: solid phase; ϕ_2: liquid phase; ϕ_3: gas phase) that represent the rate of fractional volume for each phase in a cell and these functions need to satisfy the relationship: $\phi_1+\phi_2+\phi_3=1$ ($0 \le \phi_I \le 1$) in a cell, $q=q(y,z,t)$ is wave generation source with its strength q^* assigned only at source line ($x=x_s$).

(2) Computational algorithm

Fig.1 indicates the computational flow chart of the 3-D multiphase flow numerical model. Eqs.(2) and (3) are divided into an advection step and a non-advection step by making use of a time splitting method as shown in Eqs.(7) ~ (10). The resultant equations are discretized by employing irregular staggered mesh grids. A CIP (Cubic Interpolated Propogation) method developed by Yabe and Aoki[7] is used to calculate the hyperbolic equations for all variables at the advection step, while equations at the non-advection step are solved with an extended SMAC (Simplified Marker And Cell) method[8], which can simulate both compressible and incompressible fluid. Eq.(1) is solved by a CIP-CSL2 (Constrained Interpolation Profile - Conservative Semi-Lagrangian 2) method[9], which is one of the conservative methods extended from a CIP method. The effect of surface tension on the gas-liquid interface is evaluated by using a CSF (Continuum Surface Force) model proposed by Brackbill *et al.*[10], which interprets surface tension as a continuous mass force across the interface. A LES (Large Eddy Simulation) based on a DTM (Dynamic Two-parameter Mixed) model is applied for estimating turbulence quantities[11].

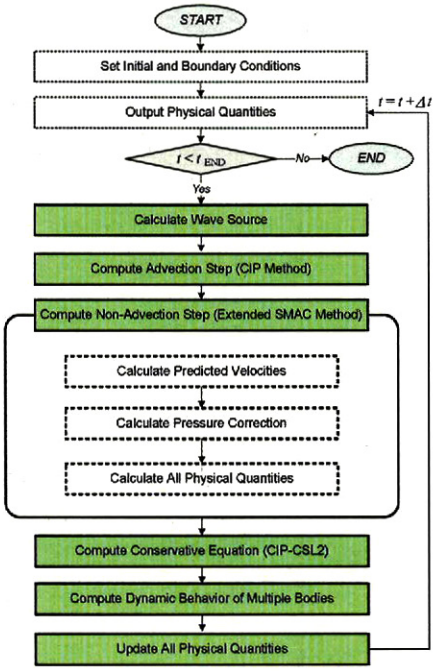

Fig.1 Flow chart of multiphase flow model

[Advection step]

$$\frac{\partial u_i}{\partial t}+u_j\frac{\partial u_i}{\partial x_j}=0 \tag{7}$$

$$\frac{\partial p}{\partial t}+u_j\frac{\partial p}{\partial x_j}=0 \tag{8}$$

[Non-advection step]

$$\frac{\partial u_i^{n+1}}{\partial t}=-\frac{1}{\rho^n}\frac{\partial p^{n+1}}{\partial x_i}-g_i+F_i \tag{9}$$

$$\frac{\partial p^{n+1}}{\partial t}=-\rho C_{ls}{}^2\left(\frac{\partial u_j^{n+1}}{\partial x_j}-q\right) \tag{10}$$

where, F_i represents external force term, such as viscous, surface tension and dissapation zone terms.

(3) Numerical procedure at advection step

The equations at the advection step are calculated by using the CIP method with 3rd-order accuracy, which can solve the advection equation precisely, taking advantage of the hyperbolic equation f as represented in Eq.(11).

$$\frac{\partial f}{\partial t}+u_j\frac{\partial f}{\partial x_j}=0 \tag{11}$$

Fig.2 shows the concept of one-dimensional CIP method, in which the spatial distribution of value is interpolated in the range of the interval $[x_{i-1}, x_i]$ with a cubic polynomial function formed as Eq.(12).

$$F_i^n(x)=a_1X^3+a_2X^2+a_3X+a_4 \tag{12}$$

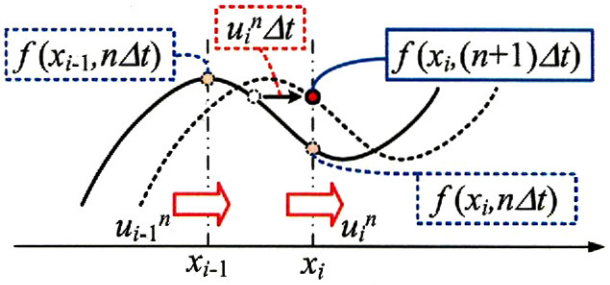

Fig.2 Concept of one-dimensional CIP method

The unknown coefficient $a_1 \sim a_4$ in the interpolation function of $F_i^n(X)$ are determined from the continuities of f and its spatial derivatives f_x at the grid points x_{i-1} and x_i. Then, value f_i^* at the next time step is computed by Eq.(13).

$$f_i^*=F_i^n(x_i-u_i\Delta t) \tag{13}$$

(4) Numerical procedure at non-advection step

Eqs.(9) and (10) cannot be solved explicitly since the unknown variables at the next time step are included in both the left and the right sides of the equations. In this model, the extended SMAC method is used to compute for both compressible and incompressible fluids.

The predicted velocity $\tilde{u}_i$ is computed explicitly by Eq.(14) with the help of variables after the advection step.

$$\frac{\tilde{u}_i-u_i^*}{\Delta t}=-\frac{1}{\rho}\nabla p^*+F_i^* \tag{14}$$

where, superscript * represents the time step after the advection step.

The Poisson equation for the pressure correction $\delta p=p^{n+1}-p^*$, which is shown in Eq.(15), is derived by eliminating $\nabla\cdot u_i^{n+1}$ from Eq.(10) using Eq.(14) and Eq.(9).

$$\nabla\left(\frac{1}{\rho^*}\nabla\delta p\right)=\frac{\delta p}{\rho^* C_{ls}^2\Delta t^2}+\frac{1}{\Delta t}\frac{\partial\tilde{u}_i}{\partial x_i} \tag{15}$$

The pressure correction δp in Eq.(15) is solved by an ILUCGS (Incomplete LU decomposition Conjugate Gradient Squared) method.

Finally, all the variables at the next time step $t=(n+1)\Delta t$ are updated by Eqs.(16) ~ (18).

$$u_i^{n+1}=\tilde{u}_i-\frac{\Delta t}{\rho^*}\nabla\delta p \tag{16}$$

$$p_i^{n+1}=p_i^*+\delta p \tag{17}$$

$$\rho^{n+1}=\rho^*-\rho^*\nabla\cdot u_i^{n+1}\Delta t \tag{18}$$

The local sound speed C_{ls} and the viscous coefficient μ for each cell are evaluated from Eqs.(19) and (20).

$$C_{ls}=\phi_1C_{ls1}+\phi_2C_{ls2}+\phi_3C_{ls3} \tag{19}$$

$$\mu=\phi_1\mu_1+\phi_2\mu_2+\phi_3\mu_3 \tag{20}$$

where the subscripts 1, 2 and 3 represent solid, liquid and gas phases, respectively.

(5) Surface tension

A CSF model developed by Brackbill *et al.* is introduced into Navier-Stokes equations to evaluate the effects of surface tension between gas and liquid phase. The CSF model assumes that the interface between gas and liquid phases, the thickness of which is in fact 0, has some transition ranges. The surface tension assumed as the body force is denoted as Eq.(21).

$$f_{si}=\sigma k\frac{\nabla\phi_2}{[\phi_2]}\frac{\phi_2}{\langle\phi_2\rangle} \tag{21}$$

where σ is the coefficient of the surface tension, k is the curvature, $[\phi_2]=1$ and $\langle\phi_2\rangle=1/2$.

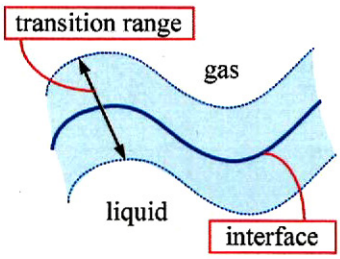

Fig.3 Concept of CSF model

(6) Dynamic motion analysis of multiple rigid bodies

The density function of solid phase for each rigid body ϕ_{1l} is introduced into the model in order

to compute the motion of multiple rigid bodies, in which l represents the order number of the bodies. It should be noted that the relationship between ϕ_1 which represents a density function of solid phase in a computational cell and ϕ_{1l} is required to satisfy Eq.(22). First, the motions of rigid bodies are simulated similarly to the numerical procedure proposed by Xiao *et al.*[12]. Assuming that rigid bodies are a high-viscous fluid, the entire computational domain including the region of rigid bodies is computed in the above-mentioned computational algorithm. However, the distortion of the rigid bodies occurs because they are treated as a fluid. To overcome this problem, the translational velocity V_l and angular velocity Ω_l at the mass center of the rigid bodies are computed by Eqs. (23) and (24). Then, the positions of each body at the next time step are calculated by applying the computed velocities U_l, which is the sum of the translational and angular velocities only to cells in the solid phase. This also indicates that the motions of rigid bodies are simulated without setting any boundary conditions between solid and other phases.

$$\phi_1 = \sum_{l=1}^{L} \phi_{1l} \le 1 \tag{22}$$

$$\frac{dV_l}{dt} = \frac{1}{M_l} \int_V \frac{d\boldsymbol{u}}{dt} \phi_{1l} \rho_{sl} dV \tag{23}$$

$$\frac{d\Omega_l}{dt} = \frac{1}{I_l} \int_V \boldsymbol{R}_l \times \frac{d\boldsymbol{u}}{dt} \phi_{1l} \rho_{sl} dV \tag{24}$$

$$R_l = x - x_{0l} \tag{25}$$

$$U_l = V_l + \Omega_l R_l \tag{26}$$

where, L is the total number of rigid bodies, M_l is total mass, ρ_{sl} is density, I_l is the moment of inertia, R_l is a position vector from the center point of the body x_{0l} to an arbitrary location x and du/dt is calculated using the pressure values within the bodies based on Newton's second law of motion.

3. RESULTS AND DISCUSSION

(1) Computational conditions

A multiphase flow model with solid-gas-liquid interaction developed by one of the authors[13], which is referred as DOLPHIN-3D (Dynamic numerical model Of muLti-Phase flow with Hydrodynamic INteractions - 3-Dimension), is used to investigate wave run-up on singular vertical cylinder. The validity of the model is confirmed through the comparison with experimental results under both moderate wave (Case 1) and extreme wave (Case 2). Wave conditions are given in **Table 1**, and the cylinder configurations are shown in **Figs. 4** and **5**. The time interval at every time step is set constant so that the Courant condition is always satisfied.

Table 1 Wave conditions

Case	Wave height H (m)	Wave period T (s)	Deep water wave steepness $2\pi H/gT^2$	Reference
1	0.030	1.00	0.02	Sanada[14]
2	0.075	0.98	0.05	Vos, L.D. *et al.*[15]
	0.090	1.07	0.05	
	0.124	1.26	0.05	
	0.170	1.48	0.05	

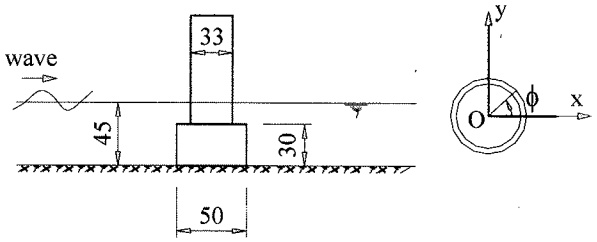

Fig.4 Configurations of Case 1, all dimension in cm

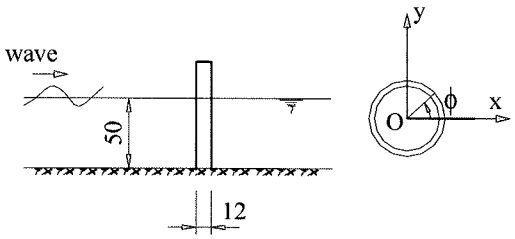

Fig.5 Configurations of Case 2, all dimension in cm

(2) Interaction of wave and fixed body

Fig.6 exemplifies the interaction of water surface and column in Case 1. As shown in **Fig.6**, the spatial distribution of water surface around the column is influenced by diffracted waves due to wave-structure interaction. One example of free surface variation and x-z cross-section velocity field along the x-axis is given in **Fig.7**. As depicted in **Fig.7**, the nonlinear effect of diffracted waves on the velocity field is confirmed.

Fig.8 shows the comparison for the spatial distribution of non-dimensional maximum water surface level $2\eta_{max}/H$ (η_{max}: maximum water surface level) around the column. A variation of non-dimensional maximum water level $2\eta_{max}/H$ along the x-axis is shown in **Fig.9**. Good agreements between the numerical and experimental results in both **Figs.8** and **9** reveal the utility and validity of the model.

The effect of wave-structure interaction on free surface and velocity field in extreme wave is also recognized from **Fig.10**. In **Fig.11**, maximum non-dimensional water surface level $2\eta_{max}/H$ for the

same deep water wave steepness $2\pi H/gT^2 = 0.5$ is presented. All the relative ratios of column diameter and wavelength D/L in Case 2 are less than 0.2, and the column is categorized as a slender structure[16], which does not have a significant influence on the wave field. But, maximum non-dimensional water surface level $2\eta_{max}/H$ larger than 1.5 reveals that strong nonlinear wave-structure interaction occurs. Furthermore, the maximum non-dimensional water surface level is larger with an increase of the wave height.

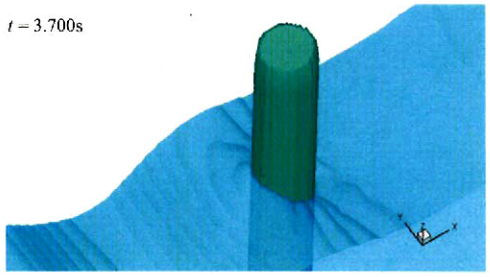

Fig.6 Interaction of water surface and column (Case 1)

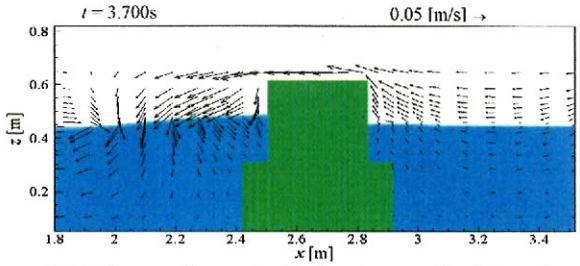

Fig.7 Free surface and velocity at x-z section (Case 1)

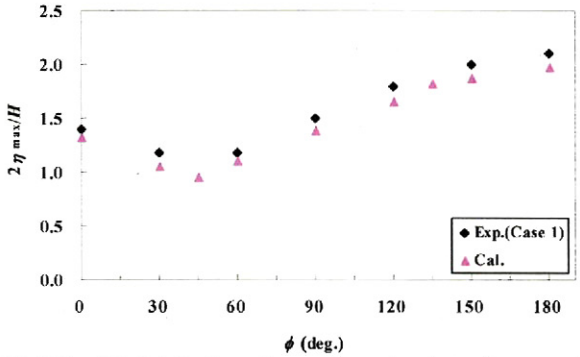

Fig.8 Spatial distribution of non-dimensional maximum water surface level $2\eta_{max}/H$ around column (Case 1)

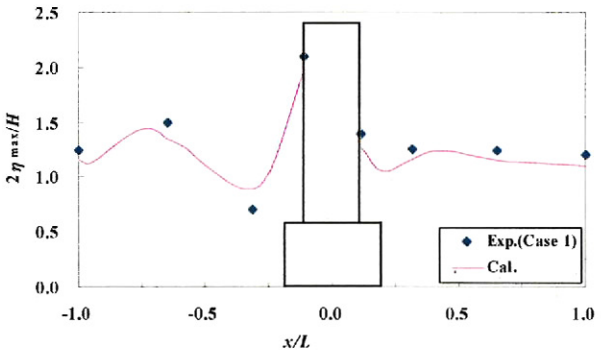

Fig.9 Spatial distribution of non-dimensional maximum water surface level $2\eta_{max}/H$ along x-axis (Case 1)

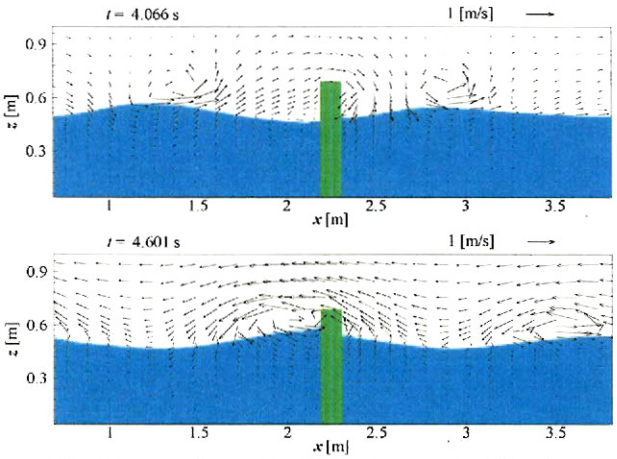

Fig.10 Free surface and velocity at x-z section (Case 2)

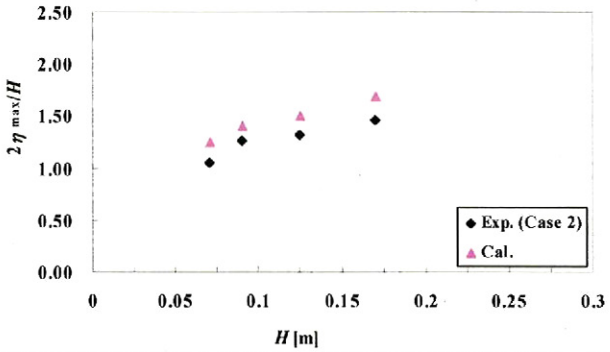

Fig.11 Maximum non-dimensional water surface level $2\eta_{max}/H$ (Case 2, Deep water wave steepness $2\pi H/gT^2 = 0.5$)

As depicted in **Fig.11**, the model is found to be capable of predicting wave run-up on a vertical column under extreme wave action through the comparison with the experimental results of Case 2.

Slight differences between the numerical and experimental results in Figs. 8 and 11 may result from the approximation of a circular column in Cartesian grids and the relationship of mesh sizes and wave parameters, which will be investigated in subsequent studies.

(3) Interaction of wave and unfixed body

In the context of simulations of nonlinear interaction of wave and body, bodies are categorized into two groups: fixed body and unfixed body (movable body under wave action). Compared with fixed body, unfixed body would be much more difficult in terms of numerical simulation. That is mainly because sophisticated techniques are needed to treat boundaries of the body and free surfaces. For the present model, this problem can be overcome by the treatment of solid body in Section 2(6). The following examination reveals the capacity of the model for simulating the interaction of wave and unfixed body.

In **Fig.12**(a), the body is initially set at a given equilibrium position in water. When the wave comes, the body is moved and turned by wave forces. Interaction of the free surface and the body is depicted in **Figs.12**(b) ~**12**(f).

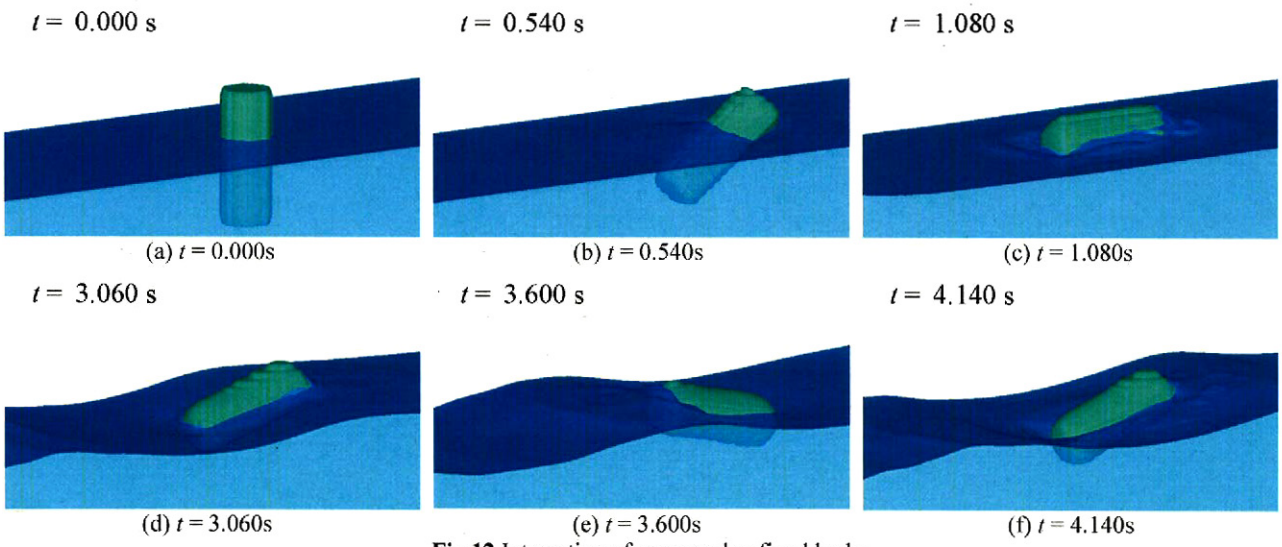

Fig.12 Interaction of wave and unfixed body

4. CONCLUSION

A multiphase flow model with solid-gas-liquid interaction "DOLPHIN-3D" was presented in this study. The model was found to be useful in investigating wave run-up on singular vertical cylinder. The utility and validity of the model was confirmed through the comparison with the previous experimental results. The model also has a function that enables to simulate physical phenomena with the nonlinear interaction of wave and unfixed body.

ACKNOWLEDGMENT: This research is supported in part by Grant-in-Aid for Young Scientist (A) (Project No.21686046, Head Investigator: K. Kawasaki) of the Ministry of Education, Culture, Sports, Science and Technology, Japan.

REFERENCES

1) MacCamy, R.C. and Fuchs, R.A.: Wave forces on piles: A diffraction theory, *US Army Corps of Engineers, Beach Erosion Board*, Tech. Memo., No.69, 1954.
2) Kim, M.H. and Yue, D.K.P.: The complete second-order diffraction solution for an axisymmetric body. Part I: Monochromatic incident waves, *J. Fluid Mech.*, Vol.200, pp.235-264, 1989.
3) Kriebel, D.L.: Nonlinear wave diffraction by a vertical circular cylinder. Part I: Diffraction theory, *Ocean Engineering*, Vol.17, No.4, pp.345-377, 1990.
4) Kriebel, D.L.: Nonlinear wave interaction with a vertical circular cylinder. Part II: Wave run-up, *Ocean Engineering*, Vol.19, No.1, pp.75-99, 1992.
5) Niedzwecki, J.M. and Duggal, A.S.: Wave runup and forces on cylinders in regular and random waves, *Journal of Waterway, Port, Coastal, and Ocean Engineering*, Vol.118, No.6, pp. 615-634, 1992.
6) Isaacson, M. and Cheung, K.F.: Second order wave diffraction around two-dimensional bodies by time-domain method, *Applied Ocean Research*, Vol.13, No.4, pp.175-186, 1991.
7) Yabe, T. and Aoki, T.: A universal solver for hyperbolic equations by cubic-polynomial interpolation I. One-dimensional solver, *Comp. Phys. Communications*, Vol.66, pp.219- 232, 1991.
8) Kawasaki, K.: Numerical model of 2-D multiphase flow with solid-gas-liquid interaction, *Int. Journal of Offshore and Polar Engineering*, Vol.15, No.3, pp.198-203, 2005.
9) Nakamura, T., Tanaka, R., Yabe, T., and Takizawa, K.: Exactly conservative semi-Lagrangian scheme for multi-dimensional hyperbolic equations with directional splitting technique, *J. Computational Physics*, Vol.174, pp.171–207, 2001.
10) Brackbill, J.U., Kothe, D.B. and Zemach,C.: A continuum method for modeling of surface tension, *J. Computational Physics*, Vol.100, pp. 335-354, 1992.
11) Salvetti, M.V. and Banerjee, S.: A priori tests of a new subgrid-scale model for finite-difference large-eddy simulations, *Physic. of Fluids*, Vol.7, pp.2831-2847, 1995.
12) Xiao, F., Yabe, T., Ito, T., and Tajima, T.: An algorithm for simulating solid objects suspended in stratified flow, *Comp. Phys. Communications*, Vol.102, pp.147-160, 1997.
13) Kawasaki, K. and Hakamata, M.: Development of Three-Dimensional Numerical Model of Multiphase Flow "DOLPHIN-3D" and Dynamic Analysis of Drifting Bodies under Wave Actions, *Annual Journal of Coastal Engineering*, Vol.54, pp.31-35, 2007. (in Japanese)
14) Sanada, M.: A study of second-approximation analysis results and application for nonlinear diffraction wave according to a large coastal structure, Doctoral thesis, Nagoya University, 223p, 1998.
15) Vos, L.D., Frigaard, P. and Rouck, J.D.: Wave run-up on cylindrical and cone shaped foundations for offshore wind turbines, *Coastal Engineering*, Vol.54, pp.17-29, 2007.
16) Sarpkaya, T. and Isaacson, M.: Mechanics of wave forces on offshore structures, Van Nostrand Reinhold (New York, London), 1981.